

ANALISIS BERBASIS SIMULASI TERHADAP SIFAT AERODINAMIKA AIRFOIL NACA 2412 DENGAN PENAMBAHAN ELEMEN FLAP DAN SLAT

SIMULATION-BASED ANALYSIS OF AERODYNAMIC PROPERTIES OF NACA 2412 AIRFOIL WITH ADDITIONAL FLAP AND SLAT ELEMENTS

Okto Dinaryanto¹⁾, Bahrul Jalaali²⁾, Syahrizal³⁾, Abdul Haris Subarjo⁴⁾, Dedet
Hermawan Setiabudi⁵⁾, Eli Kumolosari⁶⁾*

^{1,2,3,4,5,6}Department of Mechanical Engineering, Institut Teknologi Dirgantara Adisutjipto, Yogyakarta, Indonesia
email: okto.dinaryanto@itda.ac.id¹⁾, bahrul@itda.ac.id²⁾, rizalsyah224@gmail.com³⁾,
abdulharissubarjo@gmail.com⁴⁾, dedethermawan@itda.ac.id⁵⁾, elikumolosari@itda.ac.id⁶⁾*

Abstrak

Received:
14 Maret 2025

Accepted:
3 September
2025

Published:
14 Oktober
2025



Konsep awal proyek *Easy-Fly* adalah menciptakan pesawat STOL (*Short Takeoff and Landing*) yang sangat ringan dengan *drag* dan kecepatan minimal. Untuk mendukung tujuan ini, CFD (*Computational Fluid Dynamics*) atau komputasi dinamika fluida diaplikasikan dengan memvariasikan konfigurasi *flap* dan *slat* beralur tunggal serta sudut serang pada airfoil NACA 2412. Model *viscous* yang digunakan dalam kasus ini adalah *Spalart-Allmaras*. Variasi sudut serang (α) dimodifikasi pada rentang 0° – 20° . Untuk model *flap*, sudut defleksi disesuaikan menjadi 30° dan 40° , dan *slat* ditambahkan ke konfigurasinya. Berdasarkan hasil penelitian didapatkan bahwa defleksi *flap* 30° dan 40° menghasilkan nilai C_L yang lebih tinggi pada sudut serang 0° . Penggunaan desain *flap* dan *slat* pada *airfoil* NACA 2412 secara efektif menunda pemisahan aliran udara hingga mencapai sudut serang maksimum 24° . Selain desain sistem *high-lift* pada *airfoil* NACA 2412, perubahan pada *camber* dan penyesuaian garis *chord* efektif menghasilkan peningkatan yang signifikan pada koefisien *lift* (C_L), koefisien *drag* (C_D), dan sudut *stall*. Akhirnya, defleksi *flap* 30° lebih efisien daripada defleksi 40° dalam kondisi lepas landas. Rata-rata persentase kenaikan C_L/C_D dari *flap* 30° ke 40° adalah 17,61%.

Kata Kunci: NACA 2412, *flap*, *slat*, AoA, CFD

Abstract

The original concept for the *Easy-Fly* project was to create an ultra-light STOL (*Short Takeoff and Landing*) plane featuring minimal drag and speed attributes. To support this goal, CFD (*Computational Fluid Dynamics*) was applied by varying the configuration of single-grooved flaps and slats and the angle of attack on the NACA 2412 airfoil. The viscous model used in this case is *Spalart-Allmaras*. The variation of the angle of attack (α) was modified in the range of 0° – 20° . For the *flap* model, the deflection angle was adjusted to 30° and 40° , and slats were added to the configuration. Based on the results of the study, it was found that *flap* deflections of 30° and 40° resulted in higher C_L values at an angle of attack of 0° . The use of *flap* and *slat* designs on the NACA 2412 airfoil effectively delayed airflow separation until it reached a maximum angle of attack of 24° . In addition to the *high-lift* system design on the NACA 2412

airfoil, changes in camber and effective chord line adjustments resulted in significant improvements in the lift coefficient (C_L), drag coefficient (C_D), and stall angle. Finally, a 30° flap deflection was more efficient than a 40° deflection in takeoff conditions. The average percentage increase in C_L/C_D from a 30° to a 40° flap was 17.61%.

Keywords: NACA 2412, flap, slat, AoA, CFD

DOI: 10.20527/sjmekinematika.v10i2.724

How to cite: Dinaryanto, O., Jalaali, B., Syahrizal, Subarjo, A. H., Setiabudi, D. H., & Kumolosari, E., "Simulation-Based Analysis of Aerodynamic Properties of NACA 2412 Airfoil with Additional Flap and Slat Elements". *Scientific Journal of Mechanical Engineering Kinematika*, 10(2), 265-276, 2025.

INTRODUCTION

Aircraft wings are designed to produce sufficient lift to meet design requirements, thereby enhancing efficiency and cost-effectiveness in terms of travel distance and time[1]. The original concept for the Easy-Fly project was to create an ultra-light STOL (Short Takeoff and Landing) plane featuring minimal drag and speed attributes[2]. The design and examination conducted on the STOL aircraft concentrate on a high-lift mechanism[3]. The flaps and wing slats are designed to be retracted, minimizing drag during flight and achieving a very high maximum lift coefficient during takeoff and landing, which is characterized by low takeoff speeds.

Aerodynamics is the study of the air movement, especially when it interacts with a solid object, such as an airplane wing. This study is based on aircraft performance[4]. In aerodynamic analysis, understanding wing performance is a fundamental aspect of research. The basic shape of the wing depends on its primary use. For example, symmetric wings are commonly used for tails, and asymmetric wings generate lift on aircraft wings[5]. A thorough understanding of wing sections: including a summary of the airfoil data, is highly advantageous as an initial move prior to broadening the analytical scope to its 3D framework. Generally, analysis can be done in three ways: analytical solutions, experiments, and numerical approximations. It is important to note that analytical solutions are primarily effective for addressing specific, fundamental, and relatively simple problems. However, experimental approaches are often expensive and difficult to conduct. Conversely, aerodynamic numerical simulation offers a dependable approach to addressing the issues mentioned above. Currently, numerical simulation provides a reasonable means for detailed analysis of the flow around the aircraft.

Previously, experimental and numerical studies were carried out. As demonstrated in previous studies, experimental tests were used to evaluate the aerodynamics of the wing. According to research, the flow characteristics of an aircraft wing are typically obtained as pressure and velocity distributions, as well as the drag and characteristic of lift. Generally, numerical research should be done in advance to reduce the cost and time of testing. CFD (Computational Fluid Dynamics) analyses are commonly conducted to investigate aerodynamic behavior. As reported by references, one of the CFD models is Spalart-Allmaras (S-A) equation, widely used in aerospace applications[4,6,7]. The model was reliable, reasonably stable, and showed good numerical convergence in some aerodynamic properties. The S-A model calculates the kinematic viscosity transport equation but does not consider length scale calculations related to shear layer thickness.

Based on earlier research, CFD has proven to be a powerful technique for understanding physical aerodynamic characteristics. However, little study has been conducted to provide a coherent understanding of the wing aerodynamics of high-lift system simulations, and this work tries to fill those gaps [8]. The subsequent points offer a concise summary of this task. Initially, this research aimed to present the best CFD analysis methods for studying aerodynamic properties. To evaluate the aerodynamic characteristics and

achieve the required numerical accuracy, the Spalart-Allmaras (S-A) turbulence model was employed. This model was chosen due to its low computational cost and its suitability for external aerodynamic flows. To validate the numerical model, the simulation outcomes are compared with the results from wind tunnel experiments. Fourth, a numerical study was conducted on the addition of flaps and slats to the wing for lift-drag behavior. This study used the NACA 2412 airfoil. Modifications to the angle of attack (α) and the deflection angles of the flaps and slats were carried out to evaluate aerodynamic performance. Additionally, this study aims to enhance the evaluation of data-driven turbulence models for aerodynamic assessment[9].

RESEARCH METHODOLOGY

Geometry Model

This work delved into the study of wing characteristics to aerodynamic properties. A two-dimensional (2D) numerical modeling method was employed. The shape of NACA 2412 utilized was derived from publicly available information from the 4-digit NACA archive [10]. To verify the reliability of the existing CFD model for airfoil analysis, flaps and slats were added to the airfoil. The configuration applied in this study is presented in Figure 1.

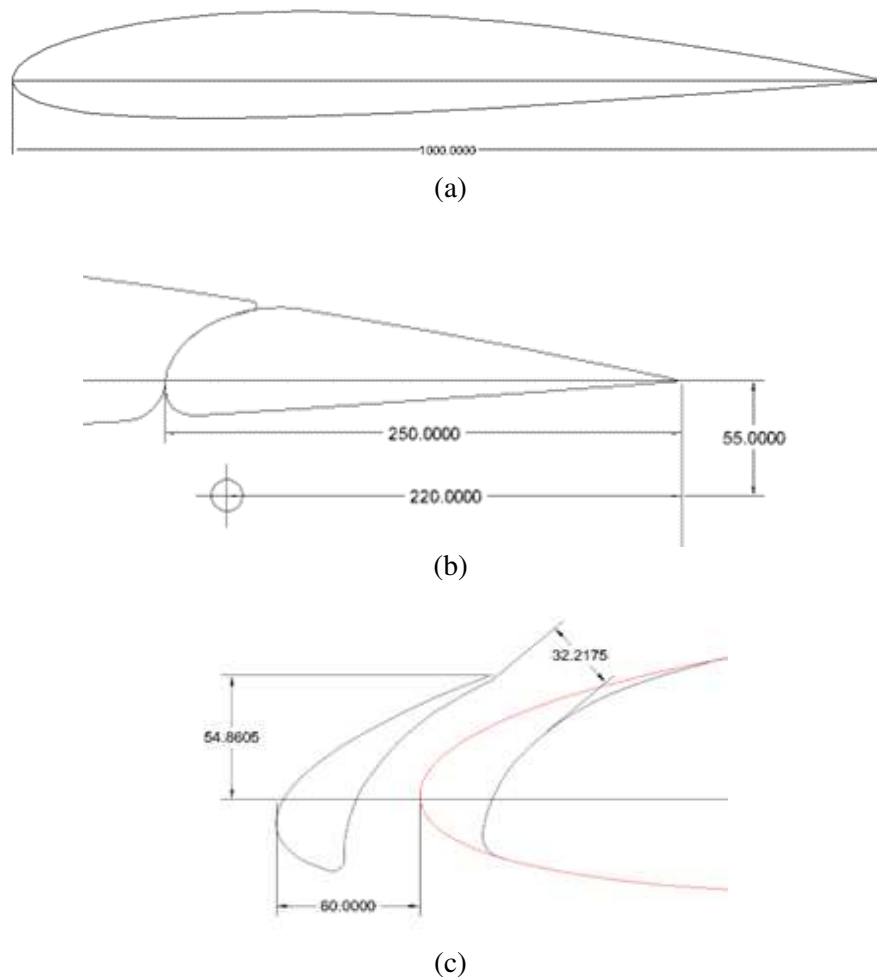


Figure. 1 (a) Standard NACA 2412 (b) Flap design (c) Slat design

The mathematical equation of the fluid analysis was conducted using mass and transport governing equations. The continuity and momentum equations, which form the basis of the governing equations, are described below.

Conservation of mass

$$\frac{\partial \rho}{\partial t} + \nabla \cdot [\rho \mathbf{V}] = 0 \quad (1)$$

Conservation of momentum

$$\frac{\partial(\rho \mathbf{V})}{\partial t} + \nabla \cdot [\rho \mathbf{V} \mathbf{V}] = -\nabla \cdot P + \nabla \cdot \tau \quad (2)$$

where ρ is the gas density, \mathbf{V} is velocity, and τ is shear stress tensor.

Equation 1 shows the conservation of mass which used in the simulation as a basic condition for solving the problem. It is related to the accuracy of the results, solution stability, and also mesh design. Equation 2 shows the conservation of momentum, which is related to the results of lift and drag force of the airfoil.

At this stage, simulation parameters including the shape of the solid surface, airflow velocity, drag force, wall treatment, and flow regime were defined. The values of the known turbulence modeling constants were obtained. Here, the angle of attack (α) variations were modified in the range of 0° - 20° . For the flap model, the deflection angle was adjusted to 30° and 40° , and a slat was added to the configuration.

Computational setup

Meshing plays a crucial role in the simulation, as a finer mesh generally leads to more accurate results. The mesh is divided into many cells, and the governing equations will be solved in each cell. Therefore, the mesh around the airfoil is finer than that to understand the aerodynamic behavior around the airfoil. It is critical because a lack of convergence and discretization methods can lead to poor simulation results. The mesh used in this study is an unstructured grid with the All-Triangles Method type with additional Refinement, which refines the grid around the airfoil, as shown in Figure 2.

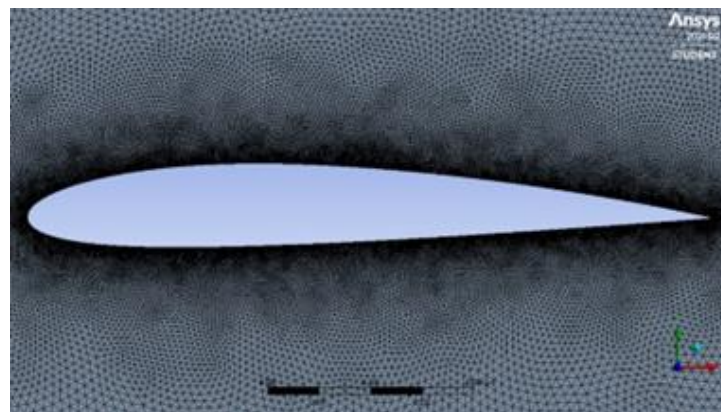


Figure 2. Meshing all triangles method

The influence of the flap and slat was accounted for by increasing the number of mesh elements on the flap structure. The mesh used exhibited a high level of smoothness, with the center span angle and smoothing controlled via height and smoothness parameters. The mesh quality is seen based on the mesh metrics in skewness with the number of elements 94160. The number of elements was obtained after the Grid Independence Test (GIT) step, as can be seen in Table 1. The target of skewness is 0.9 (Default), so the skewness is expected to be close to the target. Table 2 shows the mesh quality used for the computational study.

The absolute criteria of the residual monitors were $10e^{-5}$ and the number of iterations was 2000 since these numbers showed the convergence graph.

Table 1. Results of GIT

Number of Elements	CL	CD	CL/CD
252178	257.6337	65.55006	3.930336
94160	259.6894	65.77172	3.948345
38385	263.2276	66.86811	3.936518

Table 2. Mesh quality

Mesh Metrics	Skewness
Min	$1,4477e^{-007}$
Max	0,5459
Average	$4,6471e^{-002}$
Standard Deviation	$4,7408e^{-002}$

A CFD investigation was conducted using ANSYS-Fluent Student. The computational domain was large enough to effectively observe the wind effects on the airfoil body. As shown in Figure 3, the airfoil was positioned at the center of the domain within an atmospheric setup. During the solver stage, boundary conditions and input parameters were specified, with the airflow velocity set to 20 m/s.

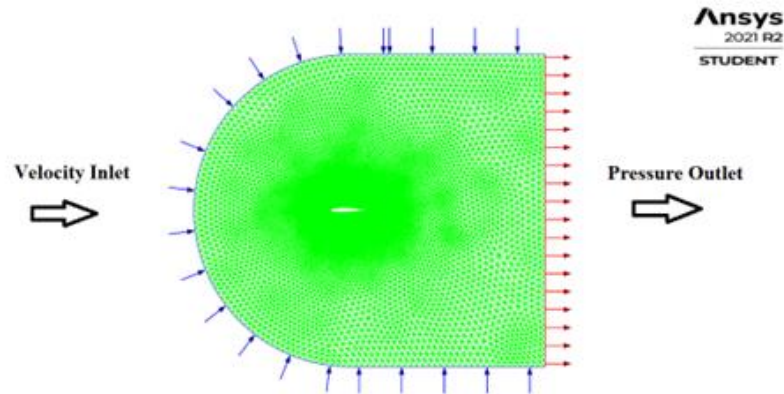


Figure 3. Computation domain and setup boundary conditions

In addition to setting steady-state and pressure-based solutions, numerical discretization was used. The vorticity-based and curvature correction addition was applied to the viscous S-A model, and the correction value was held constant by 1. The airflow was defined in the subsonic domain, the fluid was an ideal gas, and there was no heat transfer process. The surface of the airfoil was subjected to the no-slip wall boundary condition. The zero pressure and uniform velocity were established, and the turbulence properties at the inlet were configured to have a turbulence intensity of 5%. Table 3 presents the simulation setting parameters.

A constant pressure condition with a zero-velocity gradient was applied at the outlet, while open boundary conditions were set for the top and bottom walls of the domain. The pressure-velocity coupling was handled using a coupled algorithm with second-order spatial discretization. Moreover, to assess the aerodynamic characteristics, we initially concentrated on the standard airfoil. The results were subsequently compared to the experimental findings. Subsequently, we employed the flap and slat addition to assess the current method

on more intricate designs. The parametric study was conducted on different orientations of airfoils and flaps, taking into account deflection and the inclusion of slats.

Table 3. Setting parameter of the simulation

<i>Viscous Model</i>	<i>Spalart-Allmaras Model</i>
<i>Fluid</i>	Air
<i>Density</i>	1,225 kg/m ³
<i>Viscosity</i>	1,7894 x 10 ⁻⁵ kg/m-s
<i>Velocity Magnitude</i>	20 m/s
<i>Temperature</i>	288,16 K
<i>Modified Turbulent Viscosity Method</i>	<i>Second Order Upwind</i>
<i>Chord length</i>	1 m

RESULT AND DISCUSSION

Validation Study

Validation is an important step in the simulation process to determine whether the simulation results match the physical reality. The lift coefficient values obtained from the NACA 2412 airfoil CFD simulation were compared to the experimental results from wind tunnel data on the same airfoil profile, and to the Reynolds number values, as shown in Table 4. It shows that the comparison of experimental and simulated C_L values of NACA 2412 has an error value of <20%, which is 9.88% for the angle of attack 0°-18°. Therefore, the simulation results have a good agreement with the experimental results[11,12,13].

Table 4. The results of validation study

AoA	C_L		<i>Error</i>
	Experiment	Simulation	
0°	0.239	0.22829	4,48%
2°	0.456	0.45557	0,09%
4°	0.643	0.67993	5,74%
6°	0.837	0.90247	7,82%
8°	1.039	1.11839	7,64%
10°	1.233	1.32144	7,17%
12°	1.391	1.50043	7,86%
14°	1.502	1.66155	10,62%
16°	1.571	1.74715	11,21%
18°	1.196	1.62908	36,21%
MAPE			9,88%

Aerodynamics Performance of NACA 2412 Using Flap and Slat

Figure 5 shows the C_L and C_D values change for the flap deflection at the Angle of Attack 0°. The flap deflection varies from the state of the flap closed to 0°, 10°, 15°, 20°, 25°, 30°, 35°, 40°, 45°, 50°, 55°, 60°. Each increase in the flap deflection increases the value of the lift coefficient until the maximum value at the optimal flap opening, then decreases the value of the lift coefficient after reaching the highest point of its ability, namely at 40° flap deflection [14]. The value of the drag coefficient continues to increase as the flap opening increases without decreasing with each increase in flap opening. The state taking that will be discussed is in the form of 30° and 40° flap deflection by considering the efficient

C_L and C_D values for takeoff and landing conditions which are then compared between the two.

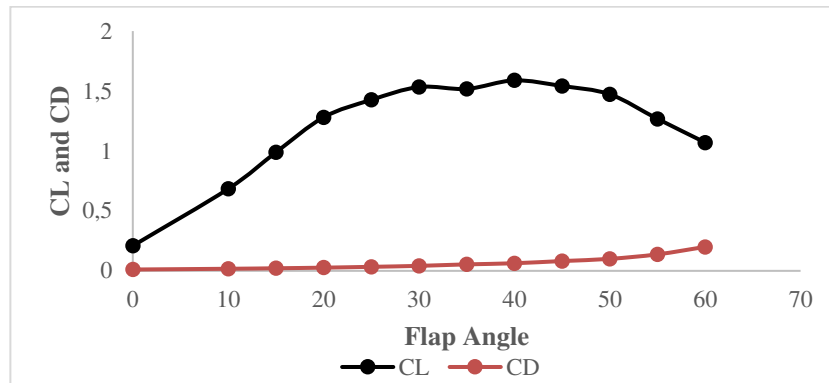


Figure 5. C_L and C_D values at various flap deflection at angle of attack of 0°

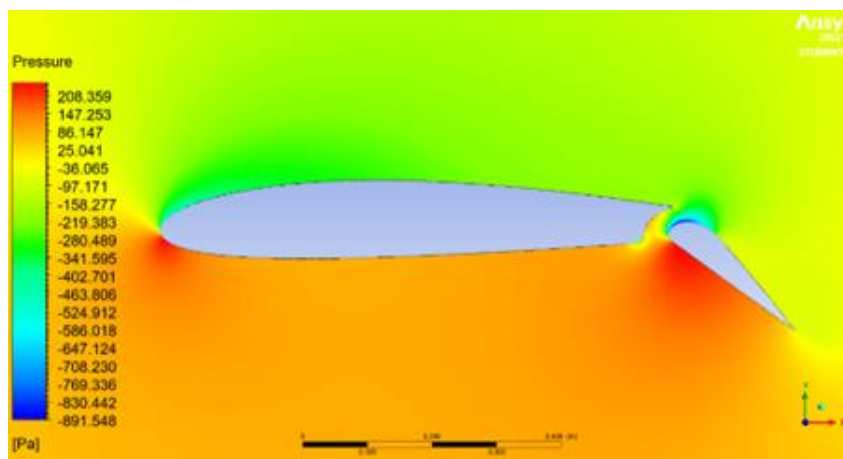


Figure 6. The contours of the NACA 2412 airfoil pressure with a flap configuration of deflection 30° and 40° at an angle of attack of 0°

Figure 6 shows the contours of the NACA 2412 airfoil pressure with a flap configuration of 40° at an angle of attack of 0° . The flap opening causes a change in the camber of the airfoil so that the pressure under the airfoil increases significantly at the 40° flap has a maximum pressure of 208.359 Pa. The pressure on the NACA 2412 airfoil occurs at a certain point with a different amount of pressure and at each point, as seen in the picture above. Greater pressure occurs on the front of the airfoil and flap because the flow slows down at points of curvature and changes direction so that the pressure in that area is greater than in other parts.

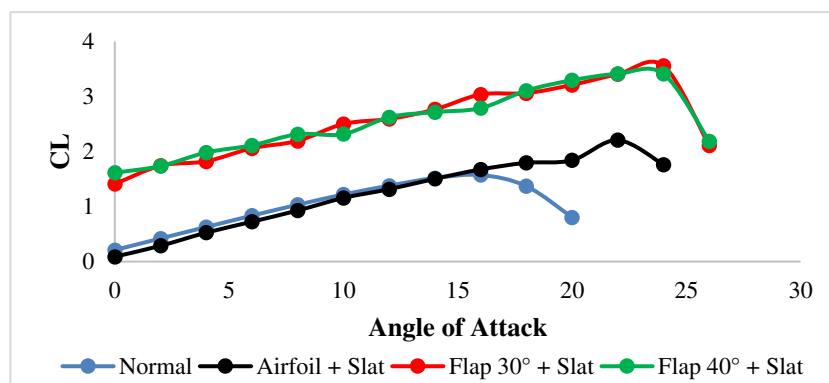


Figure 7. C_L of normal NACA 2412 airfoils, with flap and slat configurations

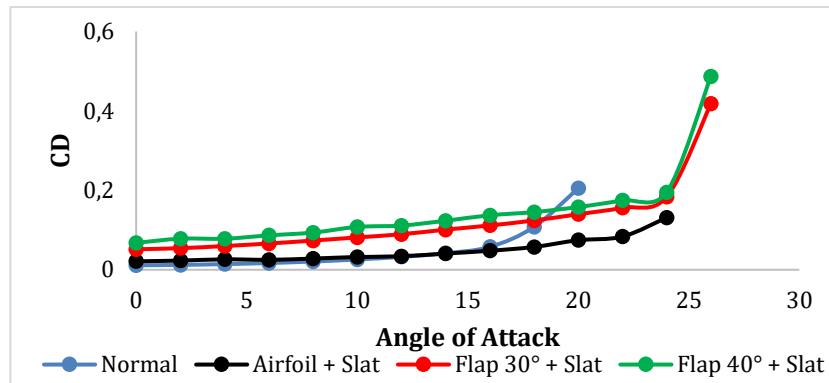


Figure 8. C_D of normal NACA 2412 airfoils, with flap, and slat configurations

To increase the angle of attack in takeoff and landing conditions, adding a slat configuration on the NACA 2412 leading edge airfoil when the flap is closed, the flap deflection is 30°, and the flap deflection is 40°. Figures 7 and 8 show a comparison of C_L and C_D values between normal NACA 2412 airfoils, additional flaps, and flap and slat configurations. Figure 7 shows that the lift coefficient with the additional slat configuration using 30° and 40° flap deflection significantly changes from the airfoil force coefficient with the slat configuration without the flap and it reached a maximum angle of attack of 24°. At low angles of attack, the slat does not affect the C_L value of the NACA 2412 airfoil. On the other hand, the C_D value is higher at a low angle of attack and lower at a high angle of attack compared to a standard airfoil, as shown in Figure 8.

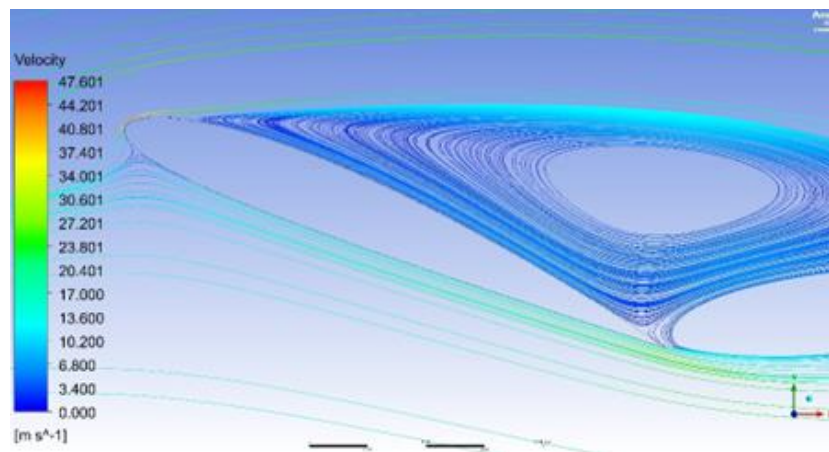


Figure 9. NACA 2412 airfoil streamline without slat at the angle of attack 22°

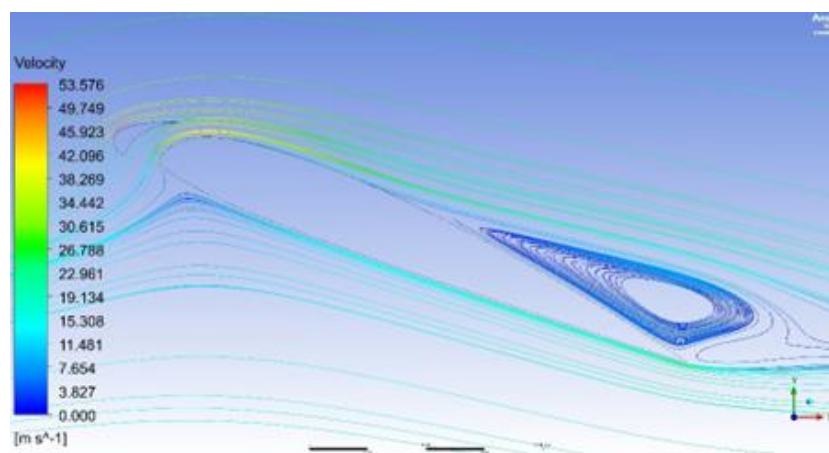


Figure 10. NACA 2412 airfoil streamline with slat at the angle of attack 22°

Figure 9 shows that there is air separation at the top of the airfoil after the airfoil breaks up the airflow. This is because the air cannot follow the shape of the airfoil surface at a high angle of attack. Adding a slat reduces the air separation in the NACA 2412 airfoil, as seen in Figure 10, where the air separation is reduced to half above the airfoil. With the addition of the slats, the angle of attack of the NACA 2412 airfoil is increased by 6° . The use of slats is one of the aerodynamic techniques for STOL aircraft. Slat is one of the tools that can increase lift by controlling the boundary layer on the aircraft wing. The added slat has a slot or distance between the slat and the airfoil. High-pressure air at the bottom of the airfoil flows to the top of the airfoil through the gap then the airflow is directed by the slat and controls the boundary layer to delay or reduce the air separation at the top of the airfoil[15]. Furthermore, it can be seen that slat significantly influences a high angle of attack. At a low angle of attack, the C_L value decreases when a slat is added compared to an airfoil without a slat, but at a high angle of attack, the slat can maintain the value C_L to exceed the normal airfoil C_{Lmax} value. C_{Lmax} increases greatly, and the stall is delayed by a large number of angles of attack[15] when the slat is applied to the airfoil with 30° and 40° flap configurations.

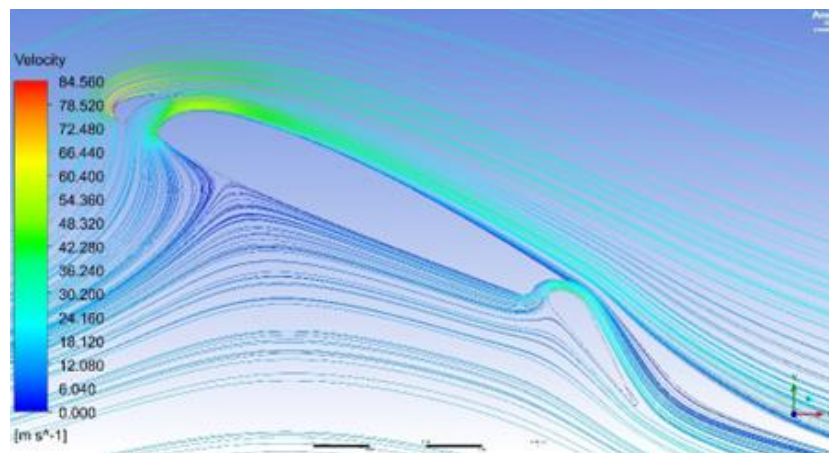


Figure 11. NACA 2412 airfoil streamline with deflection flap 30° and slat at the angle of attack 24°

The application of slats at 30° and 40° flap deflection in takeoff and landing situations at low speed of 20 m/s with an angle of attack of 24° compared to the configuration without slats can be seen from the flow pattern that occurs. The flap deflection configuration of 30° at an angle of attack of 24° shows that the air separation occurs wider at the top of the airfoil. When the slat is added, the air separation can be damped, affecting the airflow velocity around the airfoil, as seen in Figure 11. Therefore, the slat is very influential at a high angle of attack to prevent early stalls. By using slats, an increase in the angle of attack occurs when slats are applied to the aircraft wing. Therefore, additional flap and slat configurations on NACA 2412 airfoil affect the effective chord line and camber, resulting in significant increases in C_L , C_D , and stall angle values. The increase in camber affects the wing surface area, which increases the wing area and allows it to operate at low speeds.

Figure 12 shows the C_L/C_D value generated by the airfoil at each angle of attack of normal NACA 2412 airfoils, with flap and slat configurations. The Figure shows that the 30° flap deflection is more efficient than a 40° flap deflection with the addition of a slat configuration[16]. This is due to the increased lift combined with low drag and minimal flow separation at a 30° flap deflection.

The air separation in the 40° flap deflection is greater than the 30° flap deflection, both before and after the slat configuration addition, as seen in Figures 13 and 14. The difference between the two flap deflections is the separation at the back of the flap. The total separation at 40° flap deflection is greater than at 30° flap deflection, which causes a difference in the

maximum lift coefficient between the two at the same angle of attack. This becomes the advantages and disadvantages of each configuration that can be adapted to the needs and use of STOL aircraft.

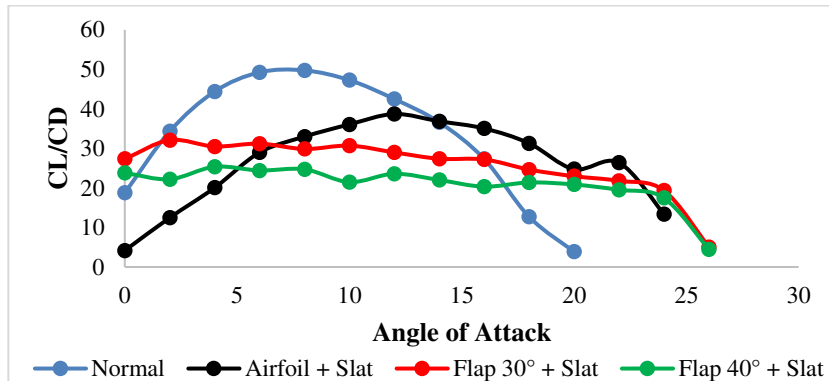


Figure 12. C_L/C_D of normal NACA 2412 airfoils with flap and slat configurations

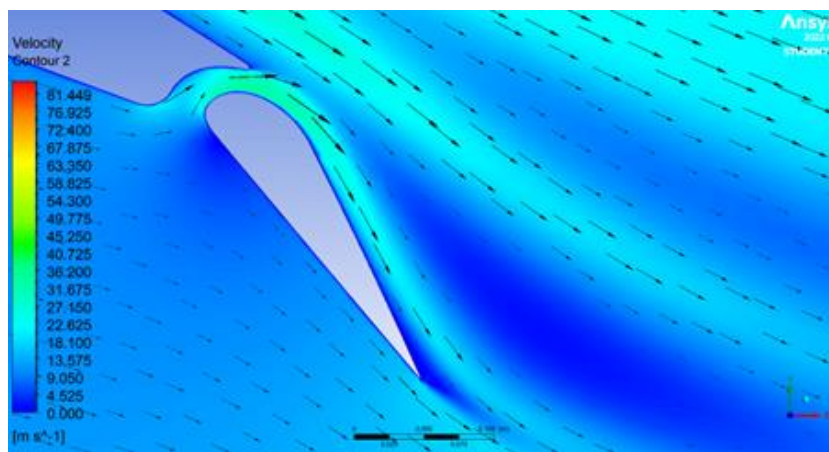


Figure 13. Contour velocity of the deflection flap 30° with an additional slat at angle of attack of 24°

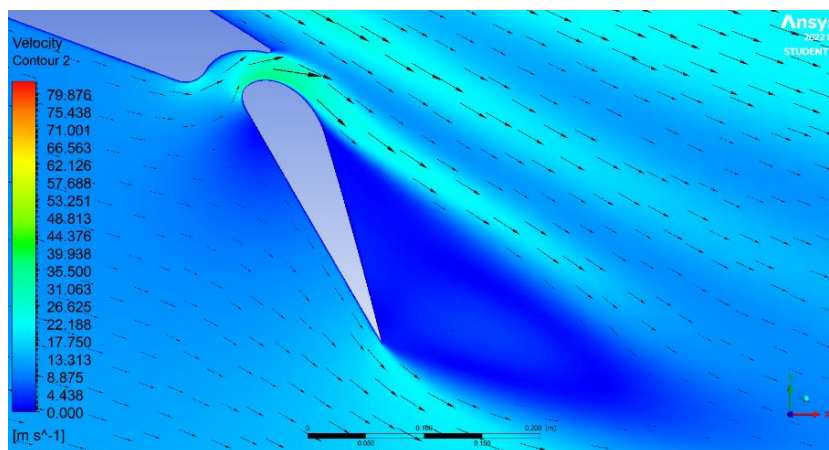


Figure 14. Contour velocity of the deflection flap 40° with an additional slat at angle of attack of 24°

CONCLUSION

The results of the CFD simulation using the Ansys Academic Student 2022 R2 software on the aerodynamic characteristics of the NACA 2412 airfoil with additional flap and slat configurations can be concluded:

1. Each increase in the flap deflection increased the value of the lift coefficient until the maximum value at the optimal flap opening, then decreased the value of the lift coefficient after reaching the highest point of its ability, namely at 40° flap deflection.
2. The application of the slat configuration can delay air separation. In the NACA 2412 airfoil without a slat with an angle of attack of 22°, the separation point occurred earlier at the front of the airfoil, with the additional slat separation point shifting backward in the middle of the airfoil. At low angle of attack, the slat did not increase the C_L value but provided additional drag on the NACA 2412 airfoil.
3. Adding flap and slat configurations on NACA 2412 airfoil affected the airfoil's camber and effective chord line, which caused a significant raise in the C_L , C_D , and stall angle values and reached a maximum angle of attack of 24°. The increase in camber affected the wing surface area, where the wing area increased so that it can operated at low speeds.
4. From the results of a comparison between 30° and 40° flap deflection with slat addition, as seen from the maximum lift coefficient and C_L/C_D ratio, it is known that a 30° flap deflection is more efficient than a 40° flap deflection in takeoff conditions. The average percentage increased from 30° to 40° flap was 17.61%.

ACKNOWLEDGMENT

The authors would like to express special gratitude to the Adisutjipto Institut of Aerospace Technology (ITD Adisutjipto) for the funding incentives for this research activity.

REFERENCES

- [1] T. M. Ichwanul H, S. P. Tirtha, A. M. P, D. Herdiana, and A. Aribowo, "Studi Eksperimental Perangkat Ujung Sayap pada Pesawat 19 Penumpang," 2020.
- [2] Z. Wang, Z. Gong, S. Mao, Z. Zhou, Y. Chen, and T. Zhang, "Short Takeoff and Landing Strategy for Small-Scale Thrust-Vectoring Vertical/Short Takeoff and Landing Vehicles," *Applied Sciences (Switzerland)*, vol. 12, no. 17, Sep. 2022, doi: 10.3390/app12178449.
- [3] J. H. Diekmann, "Flight Mechanical Challenges of STOL Aircraft Using Active High-Lift."
- [4] Y. Jang, J. Huh, N. Lee, S. Lee, and Y. Park, "Comparative Study on the Prediction of Aerodynamic Characteristics of Aircraft with Turbulence Models," *International Journal of Aeronautical and Space Sciences*, vol. 19, no. 1, pp. 13–23, Mar. 2018, doi: 10.1007/s42405-018-0022-6.
- [5] F. Liu, S. Li, J. Xiang, D. Li, and Z. Tu, "Numerical comparison between symmetric and asymmetric flapping wing in tandem configuration," *Physics of Fluids*, vol. 36, no. 4, Apr. 2024, doi: 10.1063/5.0200547.
- [6] M. Syazwan Johari, Z. M. Ali, W. Wisnoe, N. Ismail, and I. S. Ishak, "Computational Aerodynamic Analysis of UiTM's Hawkeye UAV Aircraft," *Journal of Aeronautics, Astronautics and Aviation*, vol. 53, no. 2, pp. 295–302, Jun. 2021, doi: 10.6125/JoAAA.202106_53(2).23.
- [7] S. V and I. S. R. A, "Comparative Study on the Prediction of Aerodynamic Characteristics of Mini - Unmanned Aerial Vehicle with Turbulence Models," *International Journal of Aviation, Aeronautics, and Aerospace*, 2021, doi: 10.15394/ijaaa.2021.1559.
- [8] N. Vatsa, J. C. Lin, L. P. Melton, D. P. Lockard, and R. Ferris, "CFD and Experimental Data Comparisons for Conventional and AFC-Enabled CRM High-Lift Configurations."

- [9] K. Duraisamy, G. Iaccarino, and H. Xiao, "Turbulence Modeling in the Age of Data," *Annual Review of Fluid Mechanics Annu. Rev. Fluid Mech*, vol. 11, no. 26, p. 14, 2025, doi: 10.1146/annurev-fluid-010518.
- [10] R. L. Carmichael, "Algorithm For Calculating Coordinates Of Cambered Naca Airfoils At Specified Chord Locations," 2001, [Online]. Available: <http://pdas.com>.
- [11] L. Kharulaman, A. Aabid, F. A. G. Mehaboobali, and S. A. Khan, "Research onflows for NACA 2412 airfoil using computational fluid dynamics method," *Int J Eng Adv Technol*, vol. 9, no. 1, pp. 5450–5456, Oct. 2019, doi: 10.35940/ijeat.A3085.109119.
- [12] C. Heteyi, I. Molnar, and F. Szlivka, "Comparing different CFD software with NACA 2412 airfoil," *Progress in Agricultural Engineering Sciences*, vol. 16, no. 1, pp. 25–40, Dec. 2020, doi: 10.1556/446.2020.00004.
- [13] O. John, E. Matsson, J. Voth, C. McCain, and C. McGraw, "Aerodynamic Performance of the NACA 2412 Airfoil at Low Reynolds Number," 2016. [Online]. Available: <https://www.researchgate.net/publication/319271205>
- [14] S. Srivastava CVN Aditya, "Analysis On Naca 2412 Airfoil For Uav Based On High-Lift Devices," 2016. [Online]. Available: <http://www.ijeast.com>
- [15] A. Arra, N. Anekar, and S. Nimbalkar, "Aerodynamic effects of leading edge (LE) slats and slotted trailing edge (TE) flaps on NACA-2412 airfoil in prospect of optimization," in *Materials Today: Proceedings*, Elsevier Ltd, 2021, pp. 587–595. doi: 10.1016/j.matpr.2020.10.355.
- [16] Sarjito, N. Aklis, and T. Hartanto, "An optimization of flap and slat angle airfoil NACA 2410 using CFD," in *AIP Conference Proceedings*, American Institute of Physics Inc., Apr. 2017. doi: 10.1063/1.4981179.